

Mercury Control with Calcium-Based Sorbents and Oxidizing Agents

Quarterly Report

Period of Performance:

October 1st, 2003 through December 31st, 2003

Prepared by

Thomas K. Gale

December 2003

DE-PS26-02NT41183

Southern Research Institute

2000 Ninth Avenue South

P. O. Box 55305

Birmingham, AL 35255-5305

Prepared for

Barbara Carney

National Energy Technology Laboratory

United States Department of Energy

626 Cochrans Mill Road

Pittsburgh, PA 15236-0940

Disclaimer

This report was prepared as an account of work sponsored by an agency of the United States Government. Neither the United States Government nor any agency thereof, nor any of their employees, makes any warranty, express or implied, or assumes any legal liability or responsibility for the accuracy, completeness, or usefulness of any information, apparatus, product, or process disclosed, or represents that its use would not infringe privately owned rights. Reference herein to any specific commercial product, process, or service by trade name, trademark, manufacturer, or otherwise does not necessarily constitute or imply its endorsement, recommendation, or favoring by the United States Government or any agency thereof. The views and opinions of authors expressed herein do not necessarily state or reflect those of the United States Government or any agency thereof.

Abstract

Research efforts this quarter were on continued investigations with sodium tetrasulfide injection, particularly looking at mercury removal across an ESP, rather than a baghouse. Theoretically, Na_2S_4 -injection is capable of scavenging mercury vapor from the flue gas by forming submicron-size particles of elemental sulfur in the flue gas, which react in the disperse phase before coagulating and being collected on the plates of the ESP. Results of Na_2S_4 -injection in front of a baghouse were reported in the June03 Quarterly Report. Sodium-tetrasulfide injection was very effective at removing mercury across the baghouse, and the filter cake was observed to play a significant role in the removal process. Injection atomization and droplet evaporation are less critical for removal of mercury across a baghouse filter cake than in an ESP, because all that is required is that the chemical, as Na_2S_4 and/or S° , etc., deposits on the ash cake covering the filter bags. The chemical may deposit on the filter cake before the droplets evaporate or with the ash after coagulation with flyash particles. As long as the chemical deposits on the filter cake, it is likely to be an effective sorber of mercury. However, in order to be effective for ESP applications, the chemical must form numerous fine and well-disperse particles that remain separate and suspended in the flue gas in order to reactively capture the mercury in the vapor phase, without the need for a high-contact dust cake or filter.

Experiments were performed in a 1MW semi-industrial-scale, coal-fired facility, representative of a full-scale boiler. Southern Research Institute's spike and recovery system and procedures were used to obtain real-time gas-phase mercury-speciation measurements, with less than 5% uncertainty in the measured values. Injection of sodium tetrasulfide upstream of an ESP using hot-air atomization was unsuccessful at removing vapor-phase mercury from the flue gas while the chemical was suspended in the gas. Sodium tetrasulfide injection did result in as much as 40% Hg-removal by coating the surfaces of ducting and ESP plate surfaces with the products of Na_2S_4 -injection, which coatings continued to remove mercury from the flue gas hours after injection had ceased. Flue-gas temperature and air-atomization temperature had little effect on the steady-state mercury removal. It is likely that finely dispersed S° and Na_2S_4 particles were either not effectively produced or did not persist long in the flue gas. Southern Research Institute intends to pursue future projects to develop more effective ways of dispersing the sodium tetrasulfide and increase its effectiveness at removing mercury across an ESP.

Table of Contents

Section	Page
Introduction.....	4
Experimental	5
<u>Radiant Furnace</u>	5
<u>Fuel Preparation</u>	5
<u>Burner Assembly</u>	6
<u>Convective Sections</u>	6
<u>Computer Data Acquisition and Control System</u>	7
<u>CEM System for Flue-Gas Composition</u>	7
<u>Pollution Control Equipment</u>	7
<u>Permit Equipment</u>	7
<u>Combustor Operations</u>	7
<u>Mercury Semi-Continuous Monitoring System</u>	8
<u>Spike and Recovery System</u>	8
<u>Sampling Locations</u>	10
<u>Coal Analysis</u>	11
<u>SMPS Measurements of Sub-Micron Particle-Size Distributions</u>	12
Results	13
Discussion	18
Conclusions	19
Future Work	19
References	19
Appendix A	21

List of Figures

Figure	Page
1 Combustion Research Facility (CRF)	5
2 Temperature/time history comparison	6
3 Mercury monitoring system, including spike and recovery	9
4 Mercury speciation data taken with an advanced and customized	10
5 Low-temperature Na ₂ S ₄ injection and residual effect	13
6 Effect of Higher Na ₂ S ₄ -Injection Rate	14
7 Effect of increasing flue-gas temperature	15
8 High-temperature Na ₂ S ₄ injection and residual effect	16
9 Sub-micron PSD in flue gas with and without Na ₂ S ₄ injection	17
10 Sub-micron PSD in flue gas w/wo Na ₂ S ₄ injection, while firing natural gas	17

Introduction

Most mercury control technologies (such as activated carbon injection), require baghouses (particularly for western Powder River Basin (PRB) coals), which add a significant capital and operating cost to most power plants, which typically use ESPs to collect their ash, rather than a baghouse. Hence, a technology capable of removing mercury from the flue gas before or across an ESP would be readily accepted by the coal-fired utility industry and would save electricity consumers from higher rates.

Perhaps the greatest challenge to the development of any mercury control technology for ESP applications is the trace levels of mercury in the flue gas of coal-fired boilers. Since reaction rate is concentration dependent, the reaction rate of mercury with any chemical or sorbent will be diminished by its initial low concentration and decrease further as the concentration is reduced through the capture process. Similarly, transport limitations become more severe the lower the concentration of mercury and the higher the percent removals desired. For this reason, most solutions to mercury removal involve pulling the flue-gas through a dust cake, where the contact time between the sorbent and the mercury-carrying flue gas is forced to experience intimate contact, and transport limitations are at a minimum.

Because of the obvious savings in capital expenditures that may result from a mercury control technology for ESP applications, sodium-tetrasulfide injection has been a technology of significant interest. In order for any chemical-injection or sorbent technology to work for an ESP or upstream application, the reaction rate of the sorbent with mercury must be extremely high, such that any contact of the mercury with the sorbent results in immediate capture. In addition, the sorbent must be extremely well dispersed within the flue gas, so that transport limitations are brought to a minimum, essentially eliminated.

Research efforts this quarter were on continued investigations with sodium tetrasulfide injection, particularly looking at mercury removal across an ESP, rather than a baghouse. Theoretically, Na_2S_4 -injection is capable of scavenging mercury vapor from the flue gas in part by forming many sub-micron-size particles of elemental sulfur in the flue gas, which react with mercury while suspended in the disperse phase before coagulating and being collected on the plates of the ESP. Results of Na_2S_4 -injection in front of a baghouse were reported in the June03 Quarterly Report [1]. Sodium-tetrasulfide injection was very effective at removing mercury across the baghouse, and the filter cake was observed to play a significant role in the removal process [1]. Injection atomization and droplet evaporation are less critical for removal of mercury across a baghouse filter cake than in an ESP, because all that is required is that the chemical, as Na_2S_4 and/or S° etc., deposits on the ash cake covering the filter bags. The chemical may deposit on the filter cake before the droplets evaporate or with the ash after coagulation with flyash particles. As long as the chemical deposits on the filter cake, it is likely to be an effective sorber of mercury. However, in order to be effective for ESP applications, the chemical must form numerous fine and well-disperse particles that remain separate and suspended in the flue gas in order to reactively capture the mercury in the vapor phase, without the need for a high-contact dust cake or filter.

Experimental

The Combustion Research Facility (CRF) at Southern Research Institute (SRI) in Birmingham, AL, is a 1-MW_t semi-industrial-scale, coal-fired facility, which mimics the thermal profile of a full-scale boiler from the burner through the economizer. Figure 1 shows a two-dimensional sketch of this facility.

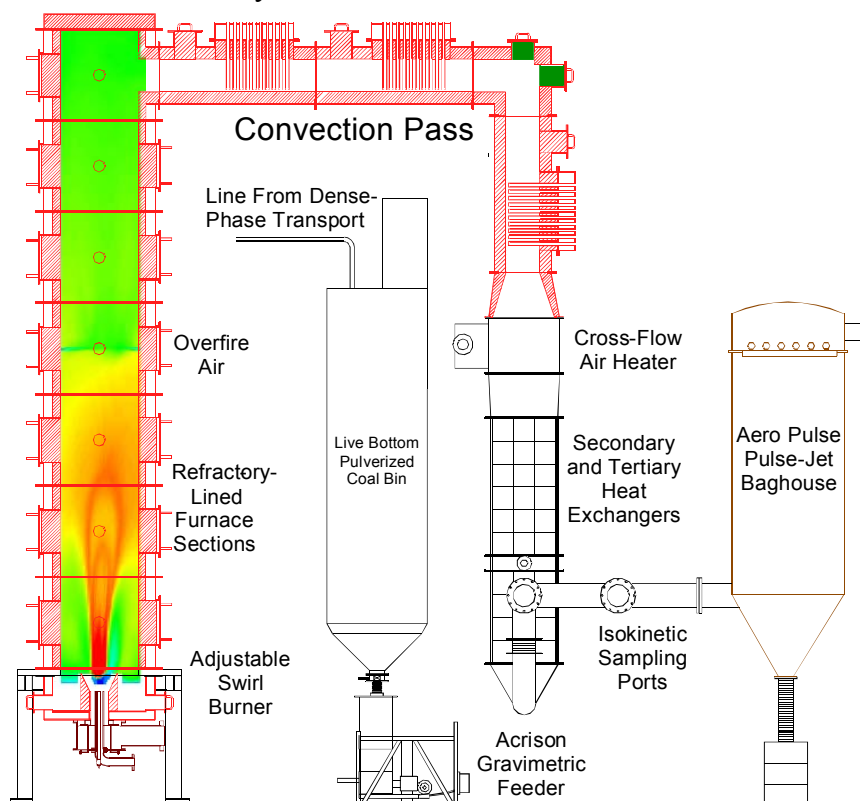


Figure 1. Combustion Research Facility (CRF).

Radiant Furnace

The furnace is a vertical, up-fired, 28-foot high cylinder, with an inner diameter of 3.5-feet (see Figure 1). This allows gas velocities of 10 to 20-feet per second and residence times of 1.3 to 2.5 seconds, depending upon the firing rate. The design furnace exit gas temperature is 2200 °F. As shown in Fig. 2, the temperature/time history of the CRF mimics that of full-scale power plants from the burner through the economizer.

Fuel Preparation

The fuel preparation area includes an open area storage yard, covered on-site storage bins, a rotary drum coal crusher, a CE Raymond bowl mill, and pulverized coal storage. The coal mill is a refurbished and instrumented Model 352 CE-Raymond bowl mill, which has a rated capacity of 2 tons per hour. This type of mill should give representative milling simulations of the different air-swept table and roller mills normally used in power plant service.

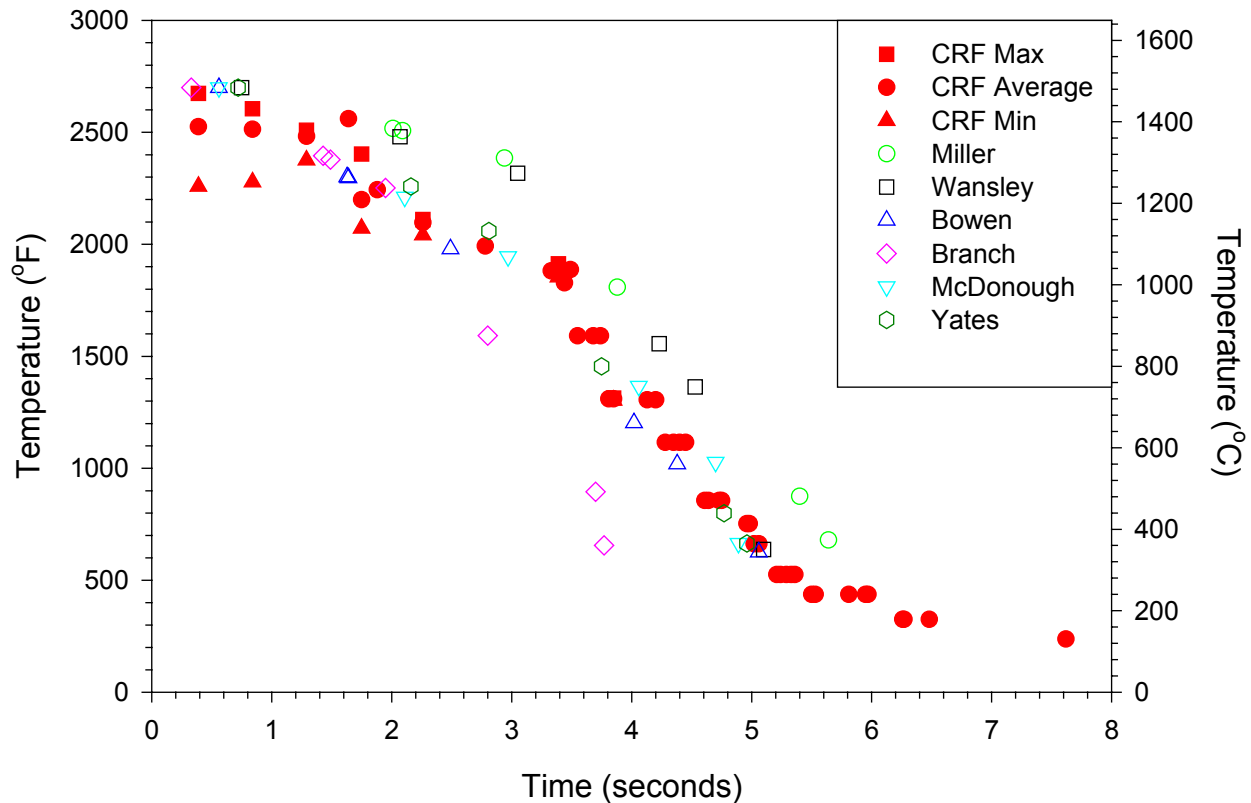


Figure 2. Combustion Research Facility (CRF) temperature/time histories compared with those of full-scale Southern Company coal-fired power plants.

Burner Assembly

The burner is mounted coaxially on the bottom of the furnace and is up-fired using natural gas, pulverized coal, any combination of the two or any other fuel that can be finely divided and transported to the pulverized coal silo. It is equipped with a flow control system for secondary air flow and a set of registers, which impart swirl to the secondary air, separate from the flow control. The secondary air and the primary air-coal mixture enter the furnace through a refractory quarl with a 25° half angle. Two clean-out ports are provided in this section, to allow bottom ash to be periodically removed from the furnace. A closed-circuit television camera with a control-room monitor allows constant monitoring of the view of the flame from the top of the furnace. A low NO_x firing system, consisting of a generic dual-register burner and an overfire air system, can be installed to simulate several combinations of low NO_x firing. The single-register burner was used for all experiments in the present investigation.

Convective Sections

The combustion gases exit the vertical furnace through a horizontal convection pass, which is designed to remove a substantial part of the heat from the flue gases. The extraction of heat was designed to simulate the time-temperature profile found in a utility boiler. A series of three air-cooled tube banks are installed in the convective pass, and the air cooling is used to control either the temperature profile of the flue gases or the tube metal surface temperatures for

fouling/ash deposition studies. A cross-flow tubular air preheater follows the convective tube banks and is used to preheat the primary and secondary air. Finally, four air-to-flue-gas recuperators are used to cool the flue gas down to a nominal 149 °C (300°F) before the flue gas enters the pollution control devices.

The convective section is 1.5 feet x 1.5 feet x 22 feet, providing gas velocities of 10 to 20 m/s (30 to 60 ft/s) and residence times of 0.4 to 0.8 seconds, again depending upon the firing rate. The design temperature range for the convective section is 1200 to 650°C (2200 to 1200°F).

Computer Data Acquisition and Control System

The facility is controlled and monitored by networked combined digital control system (DCS) and data acquisition computers, managed by Yokogawa CS-1000 system software that runs under the Windows NT operating system. This DCS performs all process control for the facility and allows complex feed-forward and calculated variable control. This computer control also performs the monitoring needed for safe operation of combustion equipment, including flame scanning and interlocks, automatic startup, and automatic shutdown of the entire facility. Process data acquisition and storage is accomplished within the Yokogawa software.

CEM System for Flue-Gas Composition

An extractive continuous-emissions monitoring (CEM) system measured the concentrations of CO, CO₂, NO_x, SO₂, and O₂ in the flue-gas exhaust. In addition, manual measurements of chlorine and moisture were obtained throughout the testing.

Pollution Control Equipment

Test equipment available for use at the Combustion Research Facility include an Electrically Stimulated Fabric Filter, a dry wall Electrostatic Precipitator (ESP), and a fluidized semi-dry / dry desulfurization system. The ESP was used for this investigation.

Permit Equipment

Particulate emissions are controlled by an Aeropulse pulse-jet baghouse, while sulfur dioxide emissions are controlled by an Indusco packed-column caustic scrubber. The pulse-jet baghouse and scrubber are required for the air quality permit of the facility issued by the Jefferson County Board of Health and are always on-line.

Combustor Operations

A routine facility operation is usually completed in one week, beginning at 8:00 am on Monday morning and ending at 5:00 PM on Friday afternoon. To facilitate start of testing on Monday morning the furnace is usually started on Sunday evening, firing with natural gas to heat up the system before switching to coal. It usually requires 12 hours before thermal equilibrium is achieved. The facility is operated 24 hours a day by two 12-hour shifts, during a test week.

Mercury Semi-Continuous Monitoring System

Mercury monitoring was performed with an advanced and customized semi-continuous Hg-speciation monitoring system. This Hg-SCEM has been customized to use an APOGEE Scientific QGIS probe for sampling flue gas. The QGIS probe is designed to pull a large volume of flue gas through an annulus within the probe at a high and turbulent velocity, thus scouring clean the walls of this annulus. The inner wall of the annulus contains a section with a porous frit through which a small sample of flue gas is drawn. The excess flue gas is directed back into the duct, downstream of the sample inlet. In this way, the QGIS probe allows a sample to be drawn from the duct without pulling it through an ash layer, thereby minimizing alteration of the gas sample – especially capture or oxidation of the vapor phase mercury by or on the particulate. Southern Research also developed a *continuous spike and recovery* system to validate the correctness of the mercury-speciation values measured. Because of these and other modifications, Southern Research Institute can now measure mercury speciation within a maximum uncertainty of 5%. Accurate and precise mercury speciation measurements are key to fundamental mercury speciation and capture investigations.

Spike and Recovery System

The *spike and recovery system* is a first of its kind prototype. The adaptation of this *spike and recovery* system to allow spiking at the tip of the APOGEE Scientific QGIS probe was performed by Southern Research personnel. The spike of mercury is introduced into the tip of the APOGEE Scientific QGIS probe far enough downstream from the inlet to prevent losses to the duct and far enough upstream of the porous annulus to allow complete mixing before the sampled gas is pulled through the porous frit. A relatively small quantity of air is used to carry the mercury spike to the probe. Therefore, dilution is insignificant, and the general flue-gas composition is undisturbed. The main impact of the spike is simply to increase the concentration of mercury in the sampled gas. This is significant, since mercury-oxidation processes that interfere with speciation measurements can involve three and four component interactions of flue-gas species on catalytic ash sites [2].

The concentration of mercury in the spike stream is generated by controlling the flow rate, pressures, and temperatures of air in and through a mercury reservoir. High-precision mass-flow controllers are used to obtain the precise metering needed for high-certainty calibrated spikes. The proper use of *spike and recovery* provides a greater level of confidence in the resulting mercury speciation measurements than other methods currently in use. A schematic of the monitoring system is presented in Fig. 3, including spike location, gas-conditioning system, and calibrated spike source.

Figure 4 illustrates the use of the *spike and recovery system* for establishing total and oxidized mercury concentrations in the flue gas, while first burning natural gas (time 0:00 to 5:00) and then Black Thunder, a Powder River Basin (PRB) coal. As shown, the *spike recoveries* are observed on top of the measured initial mercury concentrations for both fuels.

The mercury speciation data were obtained well upstream of the baghouse. Table 1 contains the Hg-speciation measurements of the PRB flue gas, after validation using the *spike recoveries* shown in Table 2 (explained below).

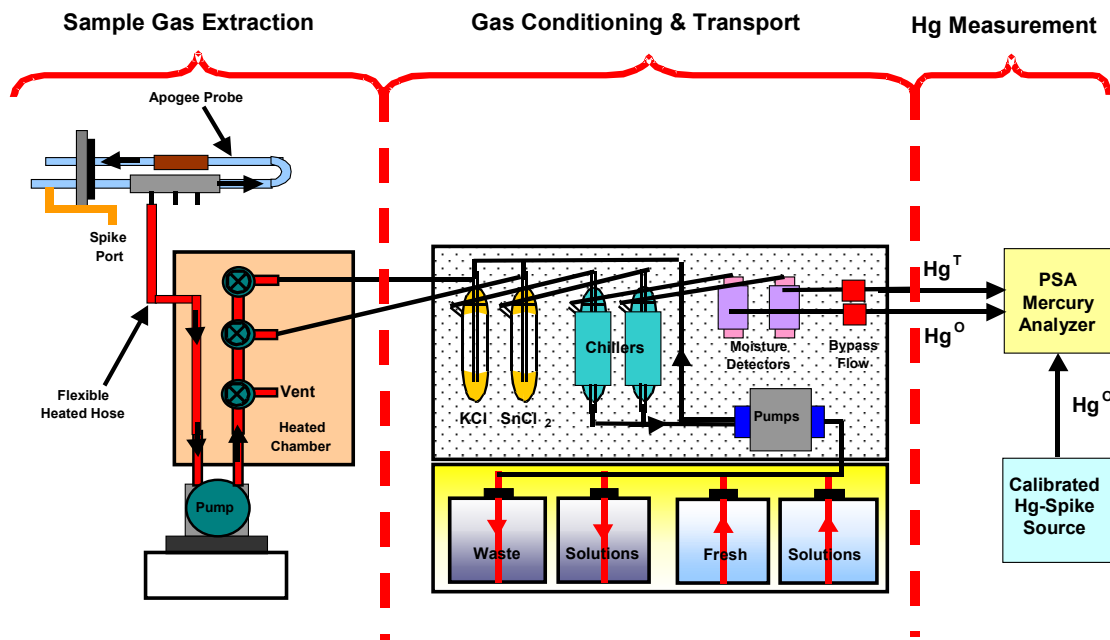


Figure 3. Mercury monitoring system, including spike and recovery.

Table 1. Location and speciation of Hg-measurements, while firing PRB coal (see Fig. 4).

Location	Temperature °C (°F)	Hg ^o ($\mu\text{g}/\text{Nm}^3$)	Hg ^T ($\mu\text{g}/\text{Nm}^3$)	Elemental Fraction %
After Recupatherm 1	260 (500)	7.4 +/- 0.93	8.4 +/- 1.1	88.1 +/- 1.5
After Recupatherm 2	163 (325)	6.5 +/- 0.44	8.0 +/- 0.70	81.3 +/- 1.0

- The mercury concentrations were measured with 6% oxygen in the flue gas.

The percentage of elemental mercury was measured directly (i.e., the population of individual measurements of Hg^o and Hg^T, taken one after the other, were used to obtain the average and standard deviation for the elemental fraction), *not calculated* from the other values in the table.

Table 2. Spike recoveries while firing PRB coal.

Sample Type	Temperature °C (°F)	Recovery 1 ($\mu\text{g}/\text{Nm}^3$)	Recovery 2 ($\mu\text{g}/\text{Nm}^3$)	Recovery 3 ($\mu\text{g}/\text{Nm}^3$)	Ave Recovery /Spike (%)
Hg ^o	163 (325)	8.30	8.78	8.06	86.4
Hg ^T	163 (325)	10.96	11.13	10.80	113.0
Hg ^o	260 (500)	7.91	8.24	7.81	82.4
Hg ^T	260 (500)	11.59	11.64	11.06	117.8

- The Hg^o spike injected into the tip of the sampling probe was $\sim 9.7 \mu\text{g}/\text{Nm}^3$.

As shown in Table 2, the recoveries of the elemental-mercury spike were consistently lower than the recoveries of total mercury, for the example shown. This was due to undesired

oxidation in the Apogee Probe and sampling lines. On the other hand, the stannous-chloride (total Hg) impingers scavenged a significant quantity of CO₂, thus artificially raising the concentration of mercury in the sample gas. However, with *spike and recovery* these errors can be observed and eliminated. In this case (see Table 2), the spike recoveries were all within 20% of the expected value.

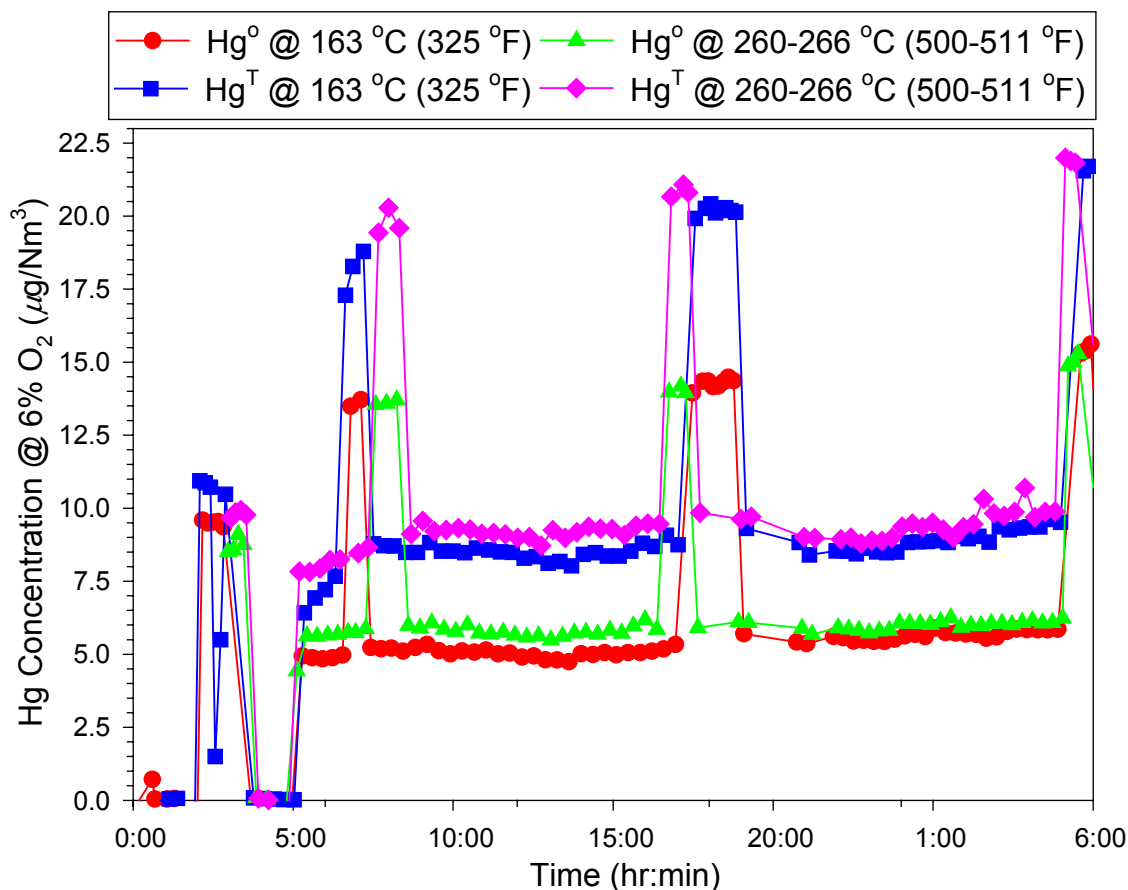


Figure 4. Mercury speciation data taken with an advanced and customized semi-continuous monitor and validated with *spike and recovery* for quality assurance.

As partially apparent in the data of Table 2, the difference in recoveries between expected and actual values was systematic, not random. In addition, as apparent in Fig. 4, there was little variation of the flue-gas measurements or the spike-recoveries themselves. Using the *spike and recovery system* has allowed mercury speciation measurements with less than 5% uncertainty for all of the data presented in this report. This estimate of uncertainty is the standard deviation of corrected values added to the inherent uncertainty of the measurement technique.

Sampling and Injection Locations

Mercury measurements were made continuously at two locations during the Na₂S₄-injection test for mercury removal with an ESP. Mercury was measured upstream of Na₂S₄-injection at a flue-gas temperature of ~550 °F. Mercury was also measured at the ESP outlet

location, just in front of the permit baghouse. This location was approximately 2 seconds downstream of the ESP. During the test, the ESP was taken out of line by diverting the flue gas directly into the permit baghouse. In this configuration, the ESP outlet mercury measurement location became the in-duct measurement location approximately 1 second downstream of Na₂S₄-injection, still directly in front of the permit baghouse. Sodium tetrasulfide was injected approximately 2 seconds in front of the ESP. However, the flue-gas temperature at this location was altered, depending on the condition desired, from 325 °F to 475 °F during the test.

Coal Analysis

Tables 3 and 4 contain the analysis (including Hg and Cl) of the North Antelope (NARC) Powder River Basin (PRB) coal used in this work.

Table 3. North Antelope (NARC) sub-bituminous coal analysis (from coal feeder discharge).

Proximate Analysis (as rec.)		Ultimate analysis (daf)		Hg and Cl Analysis (as rec.)	
% Moisture	13.00	% Carbon	74.21	Hg (μg/g)	0.06
% Ash	5.70	% Hydrogen	4.17		
% Volatiles	41.87	% Nitrogen	0.95	Cl (%)	0.013 +/- 0.013
% Fixed C	39.43	% Sulfur	0.36		
HV (Btu/lb)	9841	% Oxygen	20.32		

Table 4. Mineral analysis of NARC coal (from coal feeder discharge).

Species	NARC
% Li ₂ O	0.02
% Na ₂ O	1.8
% K ₂ O	0.52
% MgO	4.9
% CaO	21.5
% Fe ₂ O ₃	7.0
% Al ₂ O ₃	17.2
% SiO ₂	32.6
% TiO ₂	1.1
% P ₂ O ₅	0.84
% SO ₃	11.7

The general flue gas composition of major gas species was relatively constant during the entire test period, and bulk composition is given in Table 5. Unburned carbon in the ash was measured to be 0.60 +/- 0.24%, for all run conditions.

Table 5. Bulk gas composition of flue gas @ 3%O₂, unless otherwise labeled.

O ₂ actual (%)	CO (ppm)	CO ₂ (ppm)	SO ₂ (ppm)	NO _x (ppm)	H ₂ O (%)	HCl (ppmv)
7.2 +/- 0.2	81 +/- 6	17.5 +/- 0.2	170 +/- 7	183 +/- 15	8.0	1.9 +/- 1.2

SMPS Measurements of Sub-Micron Particle-Size Distributions

Real-time sub-micron particle-size distributions (PSDs) suspended in the flue gas were measured downstream of Na_2S_4 injection, at the ESP inlet and the ESP outlet, to measure the generation of sub-micron particles during hot-air atomization of sodium tetrasulfide into the flue gas. This is a particularly important measurement, because it is vital for the products of Na_2S_4 -injection (e.g., S°) to be well dispersed as a fine aerosol in the flue gas in order to be effective at removing mercury across the ESP. Appendix A contains a detailed description of Scanning Mobility Particle Sizing (SMPS).

Results

Figure 5 contains the first six data points obtained during the test in the CRF, investigating mercury removal across the ESP with Na_2S_4 injection. Each label describes the steady-state condition for the associated data point, not the point at which the condition was changed. For example, the “6.5 ppmv Na_2S_4 ” labeled data point indicates the level of mercury observed after several hours of injection, not the immediate response to the injection.

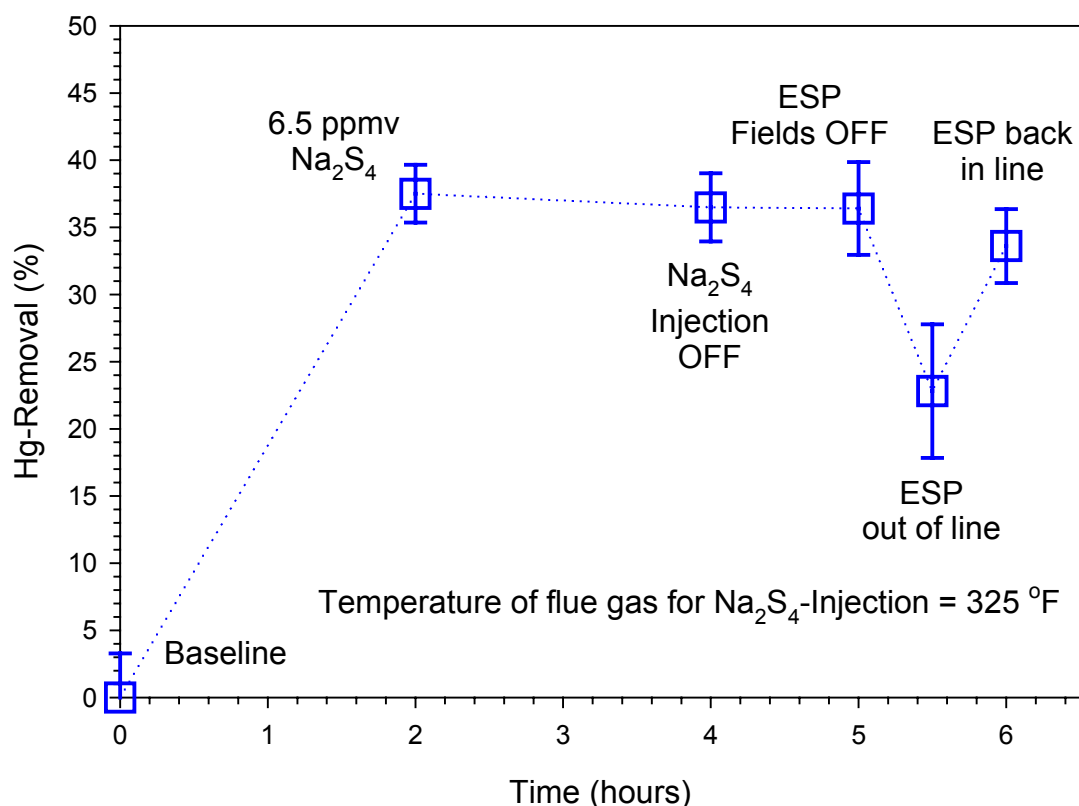


Figure 5. Low-temperature Na_2S_4 injection and residual effect.

The baseline value shown in Fig. 5 indicates that for the NARC PRB coal, very little mercury was removed from the flue gas before the exit of the ESP. This is consistent with field data and previous data taken in the CRF on PRB sub-bituminous coals, especially because the unburned carbon is generally quite low for PRB coals burned in the CRF [1, 3-8]. The temperature of the flue gas was ~ 325 °F at the Na_2S_4 -injection location for all conditions represented in Fig. 5.

Injecting sodium tetrasulfide at a rate to produce ~ 6.5 ppmv of Na_2S_4 in the flue gas resulted in the modest increase in mercury removal of $\sim 35\%$. However, when the sodium tetrasulfide injection was halted, the mercury removal remained at the $\sim 35\%$ level for hours afterward, indicating that the mercury removal was not associated with scavenging of mercury vapor by highly-reactive suspended particles. Instead, the removal of mercury from the flue gas was associated with sodium tetrasulfide and its decomposition products (primarily elemental sulfur), which had deposited on duct surfaces and on surfaces within the ESP.

In an attempt to determine the impact of ash removal in the ESP on mercury removal through the system, the ESP fields were turned off, again yielding no change in mercury removal. Following this, the ESP was taken out of line for a time and then put back in line (see the last two data points on the right of Fig. 5) with the objective of determining whether the deposited chemical responsible for mercury removal was primarily in the ducting prior to the ESP or within the ESP itself. As shown, the mercury removal dropped considerably when the ESP was taken out of line, but significant mercury removal remained. Therefore, mercury removal was likely taking place on the surfaces of the ducting before and after the ESP and within the ESP as well.

Figure 6 illustrates the effect of a higher Na_2S_4 -injection rate on total mercury removal at the ESP outlet. The first data point in Fig. 6 represents the measured mercury removal, hours after injection of Na_2S_4 (to produce ~ 6.5 ppmv) was stopped. As shown in Fig. 5, the removal of mercury during the lower concentration injection had been about $\sim 35\%$. The injection of twice the concentration of Na_2S_4 increased the observed mercury removal up to and slightly beyond the 35% Hg-removal observed earlier. However, the increase in mercury removal due to ~ 13 ppmv of Na_2S_4 was small, and turning off the injection did not reduce the mercury removal (see Fig. 6).

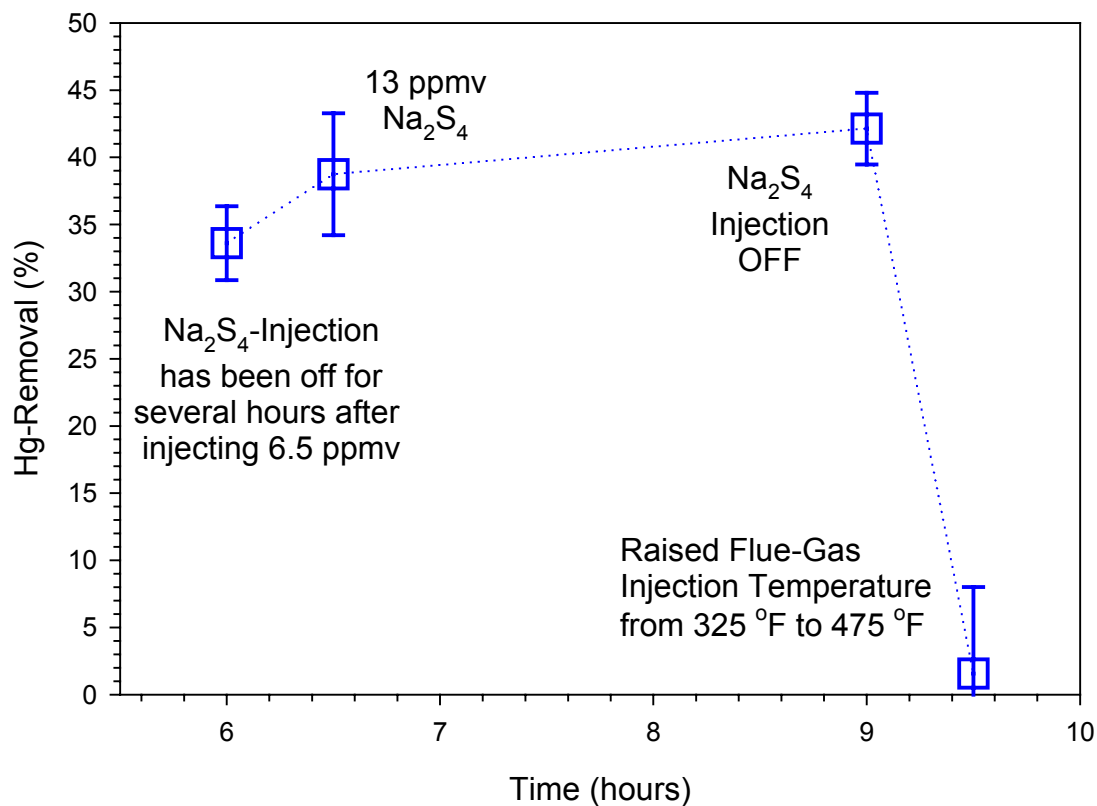


Figure 6. Effect of Higher Na_2S_4 -Injection Rate.

The fact that the mercury removal occurred on the surfaces of the duct and ESP combined with the observations that turning off injection and/or doubling the injection rate had little effect on subsequent mercury removal, suggests that the reaction was transport limited. It also suggests that the reaction of mercury with the deposited Na_2S_4 was extremely fast. Essentially, the reaction of mercury with the surfaces of the duct and the ESP was so fast that the concentration gradient of mercury in the flue gas went to zero at all such surfaces. Hence,

adding additional reactant (in the form of Na_2S_4 injection) could not enhance the rate of mercury removal. In addition, the highly-reactive coating created on duct and ESP surfaces continued to be effective at capturing all mercury that came into contact with these surfaces long after the Na_2S_4 injection had been turned off.

After the Na_2S_4 injection had been stopped and hours had passed with no reduction in mercury removal, the temperature was raised from $\sim 325^\circ\text{F}$ to $\sim 475^\circ\text{F}$ by reducing the cooling in the recuperators just upstream of injection. The increase in flue-gas temperature resulted in an immediate decrease in mercury removal, to a near zero level (see Fig. 6). As shown in Fig. 7, the transition to a new stable condition took approximately 11 hours, following the increase in temperature. The total mercury concentration was not drastically altered by the temperature increase upstream of the Na_2S_4 -injection port. However, the mercury at the ESP outlet rose immediately to concentrations similar to those measured upstream. This was probably a result of thermal liberation of mercury that had deposited earlier and was stable at the lower temperature condition, but was subsequently released when the temperature was raised.

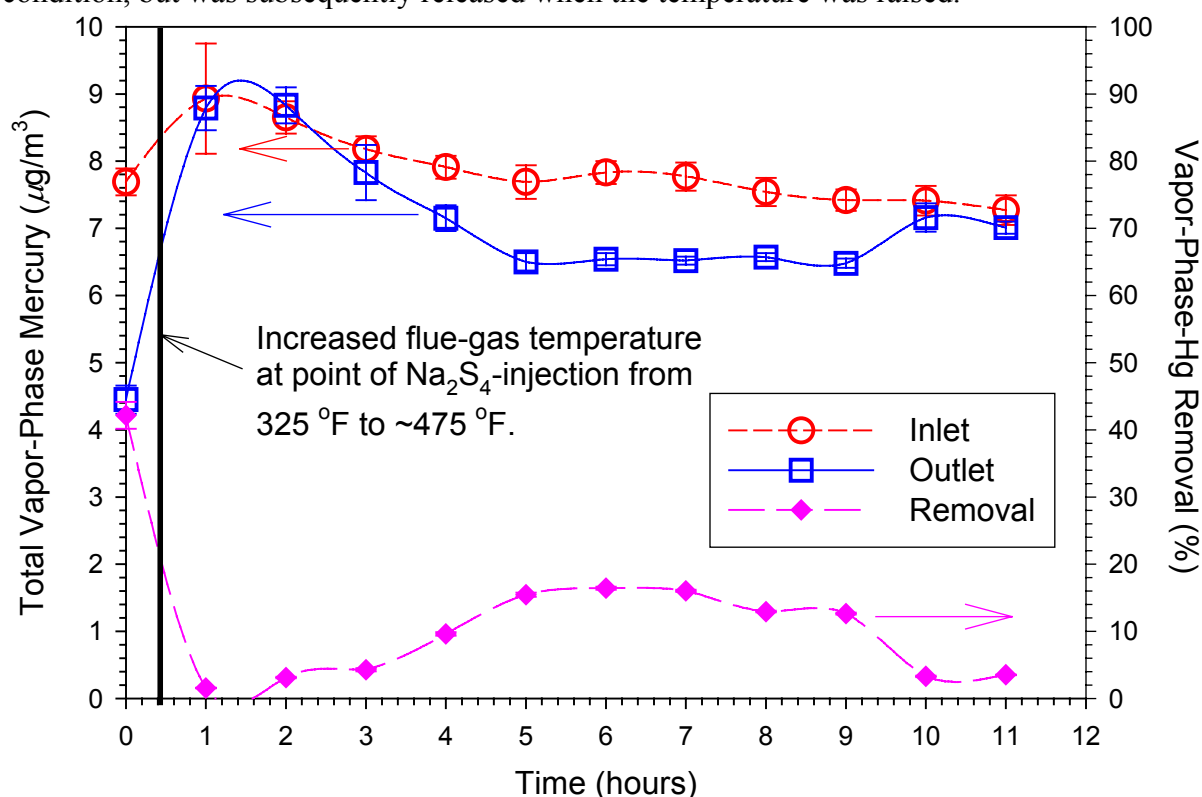


Figure 7. Effect of increasing flue-gas temperature.

Dual mechanisms probably combined to yield the initial measured results, (1) Hg-capture on the surfaces where Na_2S_4 and its products were deposited, and (2) release of previously deposited mercury from compounds that were more thermally stable at lower temperatures. After about 4 hours, it appears that the liberation of mercury began to subside, based on the fact that the total mercury measurement at the ESP outlet began to decline below the upstream concentration. It is assumed that there was still a significant residual effect of mercury removal by deposited Na_2S_4 and products on the surfaces of the duct and ESP.

After approximately 10 or 11 hours, the outlet concentration of mercury leveled out at nearly the same concentration of mercury as the upstream concentration (see Fig. 7). This was

likely due to perpetual scouring of the duct and ESP surfaces with flyash, eventually removing the deposited chemicals. At this point, the removal returned again to less than 5%.

Another test was conducted at the higher temperature, starting with a stable temperature condition, thus avoiding transitional effects. The flue-gas temperature at the location of Na_2S_4 injection was $\sim 475^\circ\text{F}$, whereas the earlier tests were conducted at $\sim 325^\circ\text{F}$. The results of this test are illustrated in Fig. 8. Again, the baseline condition produced very little mercury removal across the ESP, and injection of sodium tetrasulfide increased mercury removal to approximately the 35% level. As at the lower temperature, the ESP fields, atomizing-air temperature, and turning the injection off had little effect on mercury removal. The conclusion again was that mercury was removed by chemicals deposited on duct and ESP surfaces, and removal was transport limited.

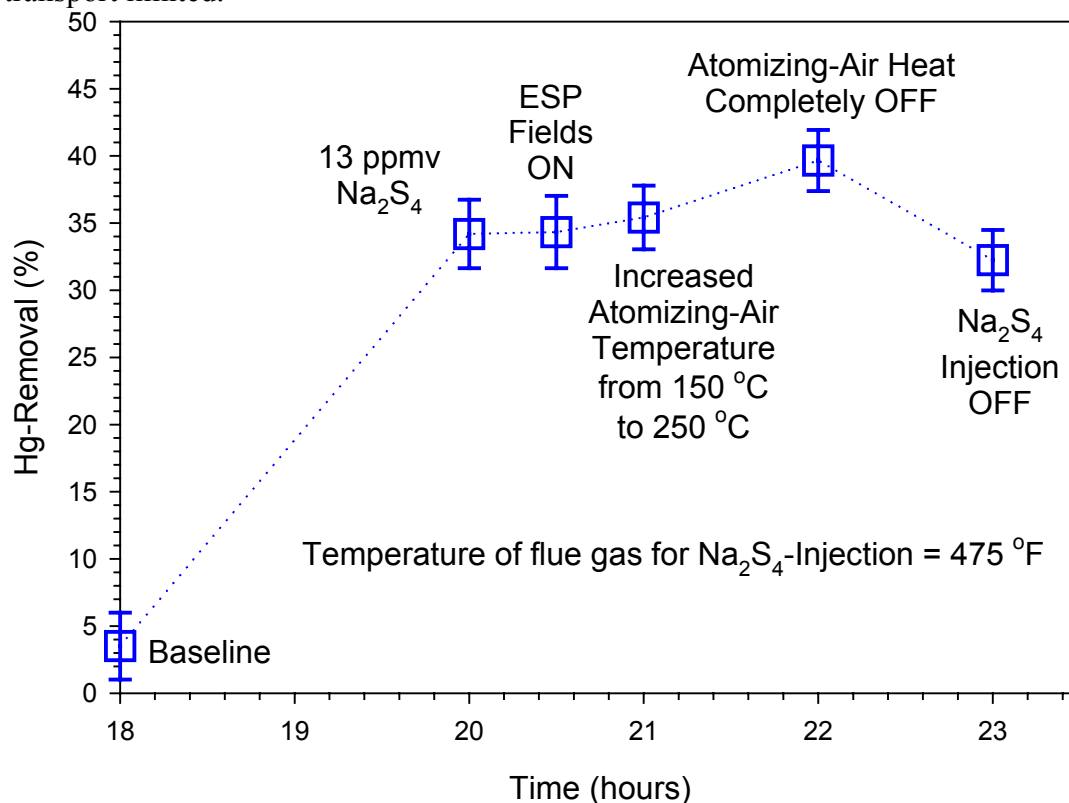


Figure 8. High-temperature Na_2S_4 injection and residual effect.

Figure 9 illustrates the results of SMPS measurements before and after the ESP, with and without sodium tetrasulfide injection. SMPS measurements gives *insitu* particle-size distributions of the sub-micron particles at a specific location in the duct. While the measurement is not hindered by the presence of larger particles, it does not measure the distribution of larger particles. These measurements were performed for the purpose of assessing the success of creating a significant concentration of disperse sub-micron sulfur particles through the hot-air-atomization of the liquid sodium tetrasulfide solution into the flue-gas duct. As shown in Fig. 9, there is not much difference between the PSD with or without Na_2S_4 injection at the inlet to the ESP.

The inherent flyash PSD makes it difficult to distinguish the generation of additional small particle loadings, so the PSD of the sub-micron particles was also measured on natural gas. Figure 10 illustrates the results of the sub-micron PSD with and without Na_2S_4 injection, while

firing natural gas. As shown, the injection of Na_2S_4 did create a sub-micron PSD. However, based on a mass balance of the amount of Na_2S_4 injected, the majority (i.e., >99%) of the sodium tetrasulfide did not form sub-micron particles, but rather formed larger particles, which were less effective for suspended-reaction with vapor-phase mercury. In an environment dominated by flyash, the sub-micron contribution by Na_2S_4 injection would have been reduced further by coagulation.

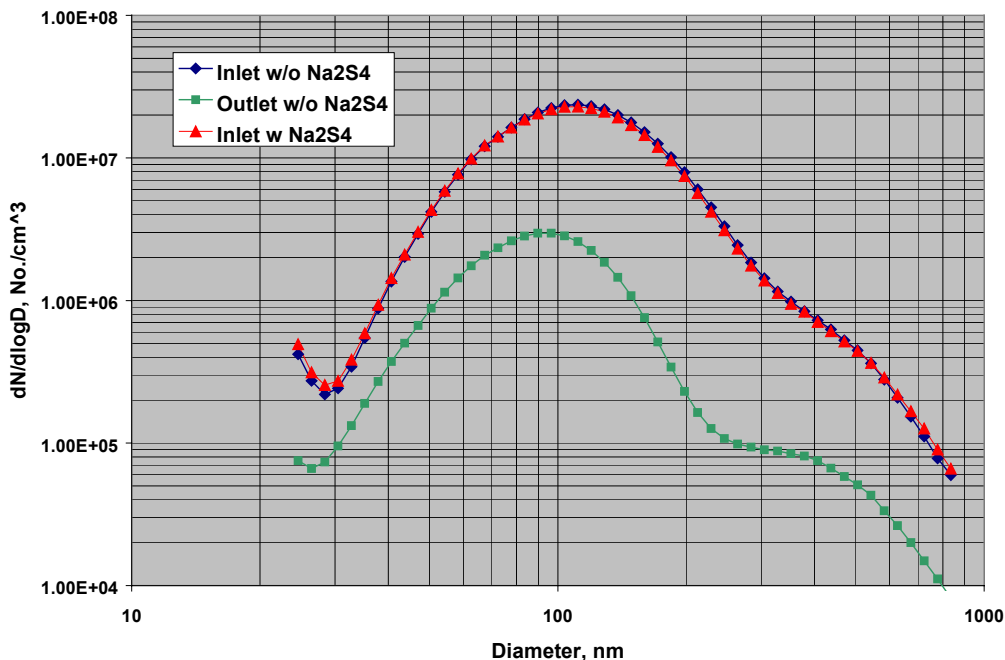


Figure 9. Sub-micron PSD in flue gas with and without Na_2S_4 injection.

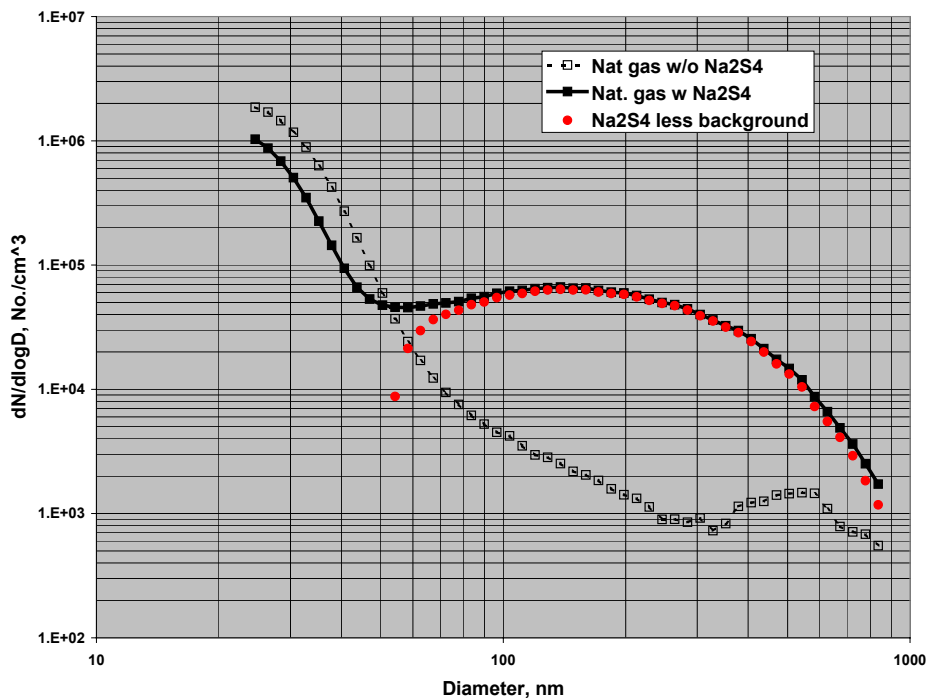


Figure 10. Sub-micron PSD in flue gas w/o Na_2S_4 injection, while firing natural gas.

H₂S measurements in the flue gas yielded small but non-zero levels of H₂S in the flue gas when sodium tetrasulfide was injected. Approximately 10% of the H₂S expected for complete Na₂S₄ decomposition was measured. This small amount of H₂S is an indicator that the expected products were in the flue gas when sodium tetrasulfide was injected. There are several possibilities why the H₂S was only 10% of that based on a mass balance, including incomplete decomposition of Na₂S₄ and reaction of H₂S with other compounds. However, the fact that some H₂S was measured indicates that enough of the desired products were present in the flue gas to remove mercury while these products were suspended in the flue gas, if these products had been highly-reactive with mercury and finely dispersed in the flue gas.

In-situ resistivity measurements were conducted to ascertain the potential impact of sodium-tetrasulfide injection on ESP performance. As shown in Table 6, the limited data obtained in the two-baseline tests and one injection test indicate that sodium tetrasulfide injection will have little effect on the ESP operation. The resistivity measured during injection falls between the two baseline measurements. Hence, the small amount of Na₂S₄ injected to mitigate mercury will not likely impact ash resistivity.

Table 6. In-situ resistivity measurements w/wo Na₂S₄-injection.

Test Condition	Spark Method	Temperature	Flue-gas moisture
	ohm-cm	°F	%
Baseline	1.70e12	292	6.1
Baseline	3.42e11	292	6.1
Na ₂ S ₄ -Injection	9.98e11	291	6.1

Discussion

It has been shown in previous work with this technology [1,7-10] and from the results discussed in this report that Na₂S₄ reaction with mercury is extremely fast. As discussed in the present report, brief injection of sodium tetrasulfide coated the surface of the duct and ESP such that removal of mercury was relatively constant for hours after injection had ceased, and mercury removal was relatively impervious to the concentration of sodium tetrasulfide injected. This requires that the mercury-capture reaction was extremely fast, such that the concentration of mercury went to zero at the reactive surfaces.

The mercury measurement results show that mercury-vapor was not significantly reduced by dispersed particles generated from the injection of sodium tetrasulfide. In addition, SMPS measurements of the sub-micron aerosol showed that sodium-tetrasulfide injection was not generating a significant sub-micron aerosol, which was necessary for the success of the technology. Although it is likely that the reactive species (Na₂S₄, S⁰, and H₂S) were present in the flue gas, because some H₂S was measured in the flue gas and removal of mercury on surfaces was significant, the disperse, suspended, fine-particle aerosol needed was not generated. There is still a possibility that more elaborate means of generating a sub-micron aerosol during Na₂S₄ injection could result in more effective mercury removal for ESP applications.

A possible reason for the less-successful generation of sub-micron particles from sodium-tetrasulfide injection is insufficient droplet evaporation. The intention of the hot-air atomization of the sodium tetrasulfide was to create a fine mist that would result in the formation of fine and reactive particles dispersed and suspended in the flue gas once the particles evaporated. However, droplet formation and evaporation kinetics resist such manipulation through

homogeneous and heterogeneous coagulation in the spray cone and with flyash particles in the flue gas. In addition, droplet persistence can be surprisingly long in the flue gas, especially if the droplets are not finely atomized.

Successful mercury removal via sodium-tetrasulfide injection upstream of an ESP may be possible by forming the submicron aerosol (with completely evaporated sub-micron droplets) before the aerosol leaves the injection nozzle. For such an injection system, hot steam may be more appropriate than hot air.

Conclusions

Sodium tetrasulfide injection with hot-air atomization was unsuccessful at removing mercury effectively across an ESP in the Southern Company pilot-facility. While as much as 40% Hg-removal on duct and ESP surfaces (coated during Na₂S₄ injection) was observed, little mercury was captured by disperse, suspended, reactive sub-micron particles, as was intended. The primary reason for this was probably a failure of the hot-air atomization injection system to produce the needed sub-micron PSD of reactive particles from evaporation of a fine mist of sodium tetrasulfide droplets. Successful mercury removal via sodium-tetrasulfide injection may be possible by forming the submicron aerosol (with completely evaporated sub-micron droplets) before the aerosol leaves the injection nozzle.

Future Work

Future work is warranted in the area of sodium-tetrasulfide injection for mercury control for ESP applications. The main objective of this future work will focus on more effective means of generating a well-disperse sub-micron aerosol during Na₂S₄ injection. This is a fairly complicated aerosol-dynamics problem, and will be aided by modeling of the aerosol-generation system and the subsequent nucleation, condensation, and coagulation that will occur in the flue gas, including interactions with the flyash. Such an effort will require fundamental design and modeling work. Experiments in the CRF used to develop such an aerosol-generation system will involve SMPS measurements while firing natural gas and subsequently during coal firing. It may be desired to dope the furnace with mercury while firing natural gas, thus allowing a two-step development process. First develop the ability to generate the desired submicron aerosol for effective mercury removal, and subsequently deal with any negative interactions associated with flyash particles. The funding for such work will be solicited in an upcoming DOE solicitation.

References

1. Gale, T. K., "Mercury Control with Calcium-Based Sorbents and Oxidizing Agents" Quarterly Report – DE-PS26-02NT41183 for period Apr. 1st through Jun. 30th, 2003.
2. Norton, G. A., "Effects of Fly Ash on Mercury Oxidation During Post Combustion Conditions", Annual Report – DE-FG26-98FT40111 for period Sept 1st, 1999 through Aug. 31st, 2000.
3. Gale, T. K., "Mercury Control with Calcium-Based Sorbents and Oxidizing Agents" Quarterly Report – DE-PS26-02NT41183 for period Jan. 1st through Mar. 31st, 2003.

4. Gale, T. K., "Mercury Control with Calcium-Based Sorbents and Oxidizing Agents" Quarterly Report – DE-PS26-02NT41183 for period Jul. 1st through Sep. 30th, 2003.
5. Behrens, G., "Final Report: An Assessment of Mercury Emissions from U. S. Coal-Fired Power Plants", No.1000608, EPRI, Palo Alto, CA (2000).
6. Gale, T. K., Merritt, R. L., Cushing, K. M., and Offen, G. R., "Mercury Speciation as a Function of Flue Gas Chlorine Content and Composition in a 1 MW Semi-Industrial Scale Coal-Fired Facility", *EPRI-DOE-EPA-A&WMA Combined Utility Air Pollution Control Symposium: The MEGA Symposium*, May (2003).
7. Gale, T. K. and Merritt, R. L., "Coal Blending, Ash Separation, Ash Re-Injection, Ash Conditioning, and Other Novel Approaches to Enhance Hg Uptake by Ash in Coal-Fired Electric Power Stations" *International Conference on Air Quality IV, Mercury, Trace Elements, and Particulate Matter*, Arlington, VA, September 22-24, 2003.
8. Gale, T. K., "Mercury Control with Calcium-Based Sorbents and Oxidizing Agents" DOE Mercury Control Technology R&D Program Review Meeting, Aug. 12-13, 2003.
9. Licata, A. and Fey, W., "Advanced Technology to Control Mercury Emissions", EPA-DOE-EPRI MEGA Symposium, Arlington Heights, IL, August (2001).
10. US Patent 6,214,304 B1, 4/10/01, "Method of Removing Mercury from a Mercury-Containing Flue Gas", J. Rosenthal, W. Schuettenheim, M. Klein, R. Heidrich, U. Nikolai, U. Soldner, assignee L&C Steinmueller GmhH.

Appendix A

Scanning Mobility Particle Sizer

The concentrations and size distributions of particles with diameters smaller than one micrometer ($1\ \mu$) can be measured and monitored in real time using a “Scanning Mobility Particle Sizer,” or SMPS. The SMPS, manufactured by TSI, utilizes size separation based on the electrical mobility of the particles followed by measurement of the concentrations of the sized particles using a continuous-flow condensation nuclei counter (CNC). The CNC detects and counts individual particles passed to it by the electrical mobility analyzer. The SMPS can be used to provide data in the form of number concentrations of particles in the diameter range from 1 nm ($0.02\ \mu$) to 1000 nm ($1\ \mu$). The upper size cut-off of the SMPS is set by an inertial impaction stage upstream of the analyzer configured to eliminate multiply-charged larger particles that would have the same mobilities as particle in the target size range. A complete concentration measurement scan of the particle size range covered by the SMPS takes about two and one-half minutes with the data and instrument operating conditions being logged by computer through each scan.

In addition, a TSI Model 3030 “Electrical Aerosol Size Analyzer,” or EAA can also be used in conjunction with a SRI “Source Extraction/Dilution System,” or SEDS, to monitor particle concentrations. The EAA is a predecessor to the SMPS that covers the same nominal size range as the SMPS but with less sensitivity, accuracy and resolution. The sample stream to the EAA is diluted as needed using dry, filtered, dilution air. Both the sample and dilution flow rates are measured using orifice meters. The diluted stream is passed through a diffusion dryer to insure that the particles are dry when measured. Although it lacks the accuracy and resolution of the SMPS, the EAA can be useful for the purpose of monitoring the stability of inlet particle concentrations at sources that do not operate in steady-state conditions.

The overall system used for source measurements with the SMPS is illustrated in Figure A1. The sample stream is first drawn through a series of diffusional absorbers utilizing activated charcoal as the absorbing medium. These absorbers, located in the duct at the probe inlet, are used to remove H_2SO_4 and other trace condensable vapors before cooling the sample streams delivered to the SMPS. (Absorbers of the same type are also used upstream of the SEDS/EAA system for the same purpose.) The sample to the SMPS, after exiting the probe, is passed through a condenser in an ice bath, to cool the sample stream and remove the bulk of the water vapor. The condenser also acts as a “time-averaging chamber” to smooth concentration fluctuations. Because the SMPS only measures a narrow range of particle sizes at any one time, short-term concentration changes must be damped to obtain reliable data on overall concentrations and size distributions. A silica-gel diffusion dryer is employed between the condenser and the SMPS so that the particles are dry when measured.

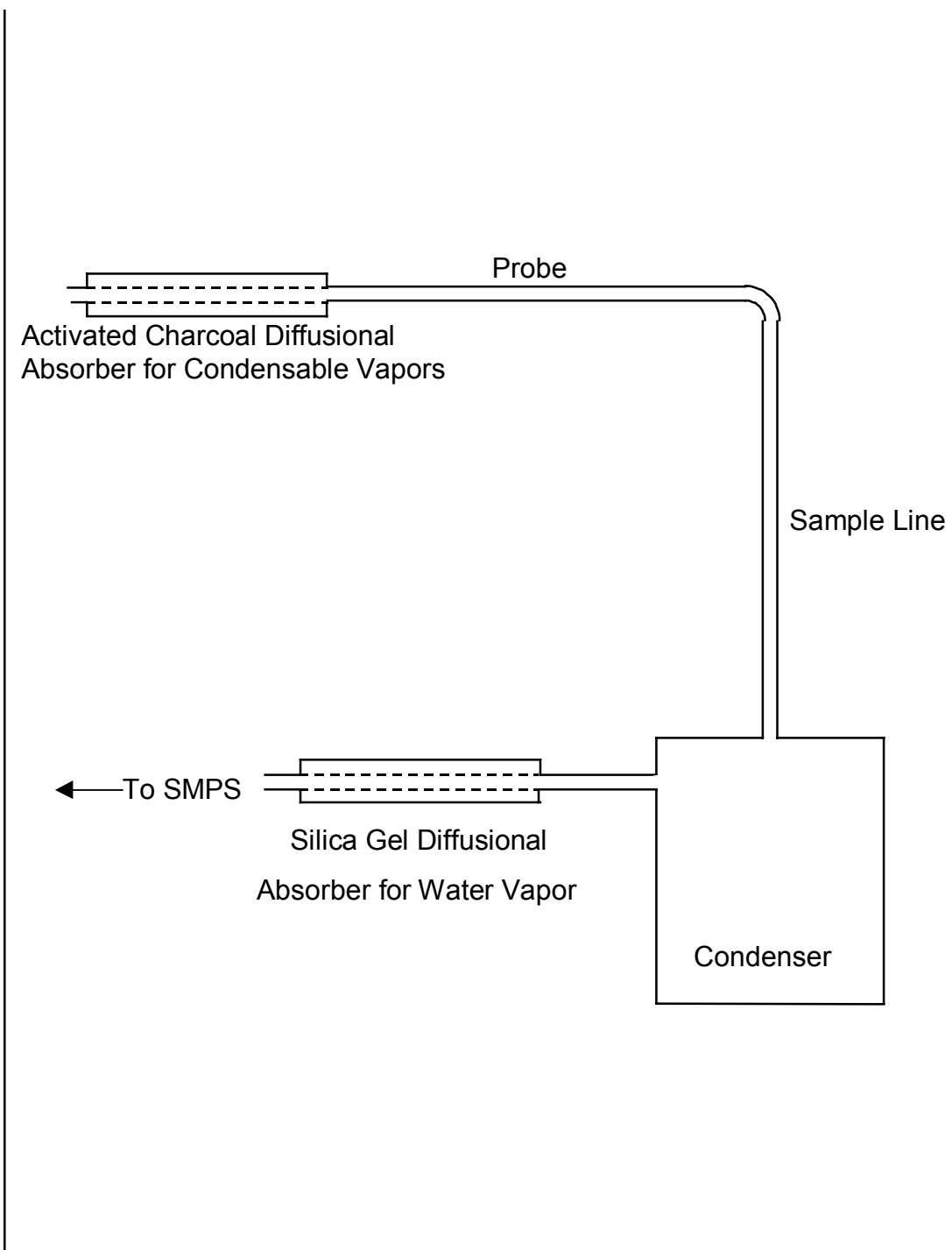


Figure A1. Schematic diagram of the SMPS source measurement system.

The SMPS system is illustrated in Figure A2, below. The sample stream is passed through an impactor to eliminate particles larger than the range to be measured and is then passed through a zone of ionizing radiation that drives the aerosol to charge equilibrium. The particles are then passed through a cylinder/pipe precipitator in which they are separated by their electrical mobility. Particles having a selected narrow range of mobilities are drawn off near the

base of the mobility separator where they are passed to a continuous-flow, condensation particle counter (CPC). In the CPC the sample stream is saturated with a working fluid and then cooled. On cooling, the fluid vapors condense on the particles, making all of them large enough to be detected by light scattering. The concentrations of the “grown” particles are then counted by conventional single-particle, optical particle counting techniques. The particle counter used in the system can cope with concentrations up to about 10,000 particles per cubic-centimeter (10^{10} particles per cubic meter). Because only a very narrow band of particle sizes are measured at one time and only a portions of the particles are charged, the total concentration at the inlet to the system can be much higher.

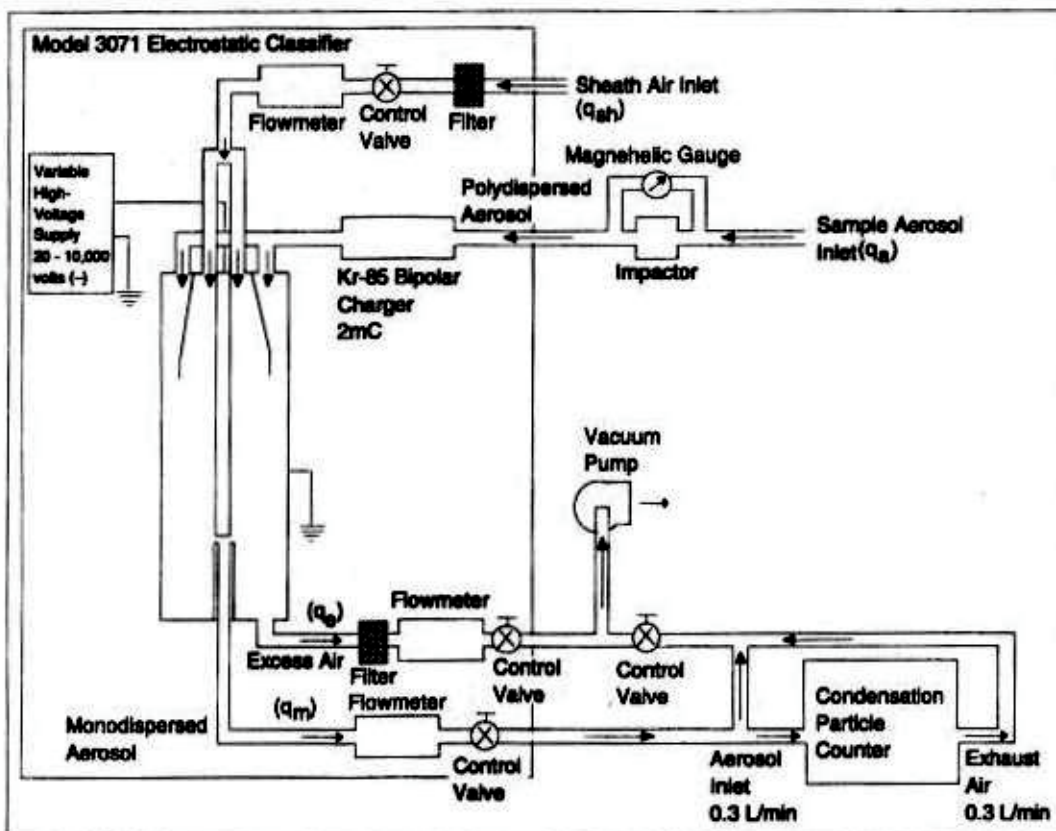


Figure A2. Schematic diagram of the SMPS sub-micron particle measurement unit.

Figure A3 below, illustrates the operation of the Scanning Differential Mobility Analyzer (SDMA), a central part of the SMPS system. The sample stream, at charge equilibrium, is passed into the analyzer at the outer periphery of the cylindrical analyzer while filtered, clean air at a matching velocity is passed through the core of the cylinder. The gas velocities are such that turbulence is minimal within the cylinder. A high-voltage power supply is used to establish an electric field between the rod and the outer wall of the analyzer. Charged particles move from the outer flow toward the center rod at rates that depend on their size and the strength of the electric field. If they are small enough, they collect on the rod upstream of an annular sample take-off slit near the bottom of the rod. Particles with the correct mobility are withdrawn in a small take-off flow through the annular slit while larger particles remain entrained in the main analyzer flow and are carried out in the “excess” air-flow. The size of the particles collected in the stream at the

annular slit can be selected by varying the voltage between the rod and the analyzer wall. When used for particle size analysis this voltage is swept from a few volts to several kilovolts in a series of pre-programmed steps, resulting in measurements being made at a pre-selected, continuous set of particle sizes over the operating range of the instrument.

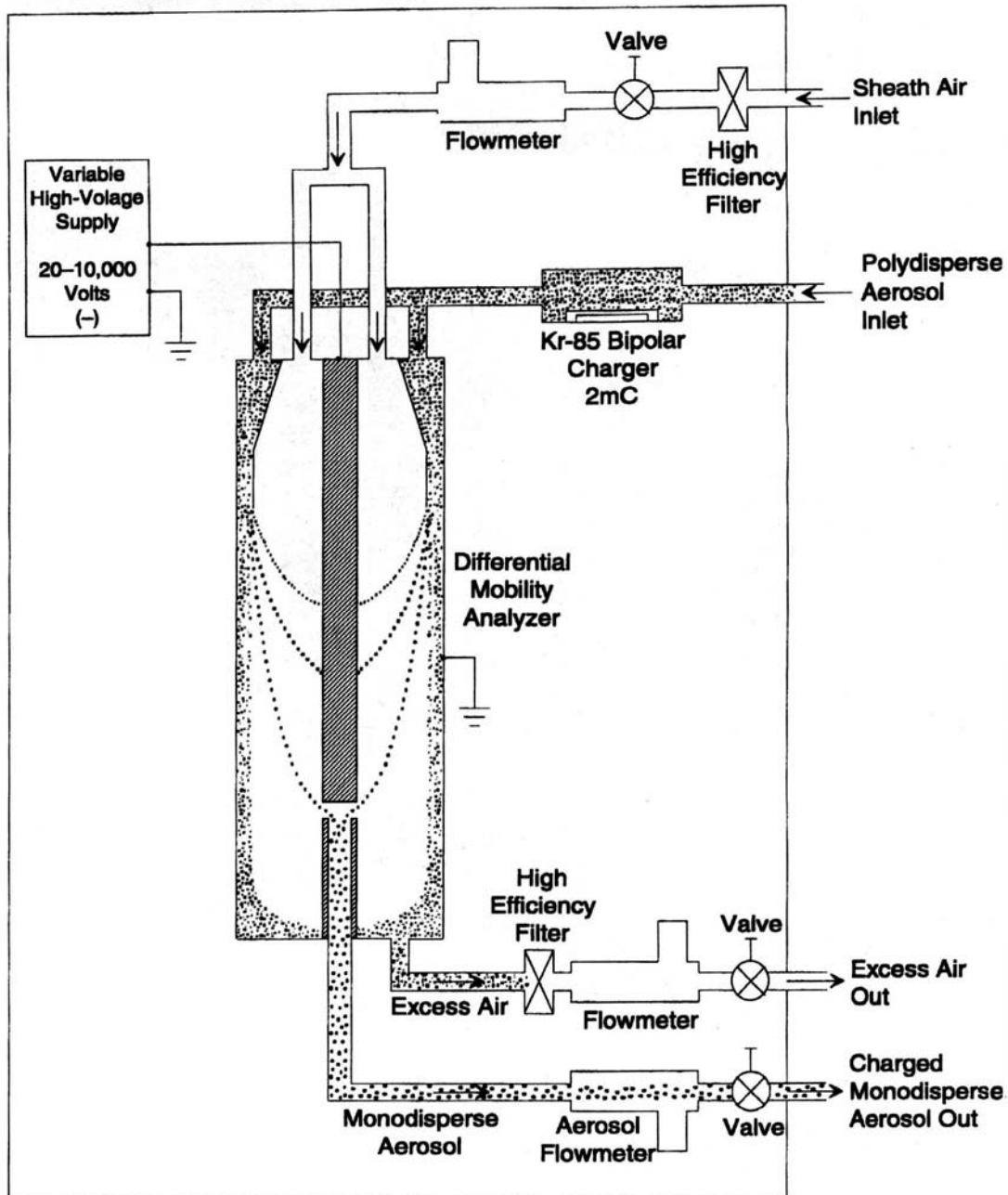


Figure A3. SDMA component operation of the SMPS mobility classifier.